US-APWR

RCCA Insertion Limit Load Test Report

Non-Proprietary Version

March 2011

Revision History

Revision	Date	Page	Description
0	March 2011	All	Original issued

Mitsubishi Heavy Industries, Ltd.
16-5, Konan 2-chome, Minato-ku
Tokyo 108-8215 Japan

Abstract

The reactor of the US-APWR is designed to produce a thermal output of 4,451MWt, which is inherited from the first Japanese Advanced Pressurized Water Reactor (J-APWR). The increase in thermal margin is attributed to an extension of active fuel length from 12ft for the J-APWR to approximately 14ft for the US-APWR. The US-APWR is a four loop PWR plant with 257 fuel assemblies having 17x17 fuel rod arrays and 69 rod cluster control assembly guide tubes (here after guide tubes). The basic design features of the US-APWR reactor internals evolved from both operating four loop plant technologies and the J-APWR.

From the safety analysis design requirements for the US-APWR internals, the Rod Cluster Control Assemblies (RCCAs) are to be gravity-inserted into the fuel assemblies without impediment after an unanticipated accident, or a seismic and postulated LOCA event. The guide tube (GT) provides horizontal restraint and guidance to the control rods and drive rod assembly. The Lower Guide Tube (LGT) in the reactor internals are subjected to large hydraulic cross-flow loads near the core barrel outlet nozzle during the LOCA event. These large LOCA cross-flow loads can produce a permanent beam-mode type deformation after the LOCA event. To ensure that the RCCAs can be gravity-inserted after permanent deformation of the LGT, a mockup mechanical test was conducted and detailed elastic–plastic finite element analysis (FEA) was performed.

This report documents the determination of the allowable hydraulic cross-flow load that assures gravity-insertion of the RCCA into the reactor core. This cross-flow load is called the “RCCA insertion limit load” in this document. The mockup test section simulated the RCCA driveline of the US-APWR reactor internals, which included the main components, such as guide tube, fuel assembly, and control rod drive mechanism (CRDM). The test was performed in air under the room temperature (RT) conditions. This test was conducted to obtain the correlation data between the LGT deformation and the RCCA insertion drag force. Based on the test results, RCCA insertion analysis was performed to determine the limiting deflection of the LGT that allows the RCCA to be inserted into the core. Finally, from elastic-plastic FEA with the use of general purpose FEA code “ABAQUS,” the RCCA insertion limit load at the operating temperature was determined.

From the results of the RCCA insertion limit load test for US-APWR, the following conclusions are drawn:

(1) The RCCA insertion limit load at the operating temperature is [ ] lbs.

(2) It can therefore be concluded that when the maximum LOCA loading is less than the RCCA insertion limit load of [ ] lbs, the RCCA can be inserted without impediment through the LGT after the postulated LOCA event.

Table of Contents

List of Tables

List of Figures

List of Acronyms

APWR	Advanced Pressurized Water Reactor
CRDM	Control Rod Drive Mechanism
FA	Fuel Assembly
FEA	Finite Element Analysis
GT	Guide Tube
J-APWR	Japanese Advanced Pressurized Water Reactor
LCSP	Lower Core Support Plate
LGT	Lower Guide Tube
LOCA	Loss of Coolant Accident
PWR	Pressurized Water Reactor
RCCA	Rod Cluster Control Assembly
RT	Room Temperature
UGT	Upper Guide Tube

1. INTRODUCTION

1.1 Objective

This document is the evaluation report of the guide tube limit load for the RCCA insertion based on a mockup test for the US-APWR.

1.2 Background

The reactor of the US-APWR is designed to produce a thermal output of 4,451MWt, which is inherited from the first Japanese Advanced Pressurized Water Reactor (J-APWR). The increase in thermal margin is attributed to an extension of active fuel length from 12ft for the J-APWR to approximately 14ft for the US-APWR. The US-APWR is a four loop PWR plant with 257 fuel assemblies having 17x17 fuel rod arrays and 69 rod cluster control assembly guide tubes (here after guide tubes).

The basic design features of the US-APWR reactor internals evolved from both the current operating four loop plant technologies and the J-APWR. The design of the core barrel assembly, with a lower core support plate, is based on the current four loop plants with a 12 ft core. In the US-APWR, the axial length of the core barrel is maintained. The diameter of the core barrel for the US-APWR is approximately 20% larger than that of the current four loop plants. This increase is necessary to accommodate an increase in the numbers of fuel assemblies from 193 to 257 and the additional space for the neutron reflector. The design of the US-APWR upper reactor internals assembly is based on the “Inverted top hat upper internals” configuration in the current four loop plants. The diameter of the upper plenum is increased by approximately 20% from that in the current four loop plants but the height of upper plenum is maintained. The cross-flow area near the outlet is therefore increased from that of the current four loop plants. As a result, the flow rate is increased, and the rated cross-flow velocity in the upper plenum is higher than that in the current four loop plants.

The GTs provide horizontal restraint and guidance to the control rods and drive rod assembly, as well as allow the parking of the drive rod during removal and installation of the upper reactor internals. All GTs are designed for removal and replacement in the event they sustain damage during operation or refueling. The height of the LGT is the same as that in the current four loop plants but the height of the Upper Guide Tube (UGT) is extended by approximately 11.8 in. with a 14 ft core. From the safety analysis design requirements and limits for the US-APWR internals, the RCCA are to be inserted without impediment after an unanticipated accident, or a seismic and postulated LOCA event. In particular, the LGT is subjected to high cross-flow loading during the LOCA event, which can produce a beam-mode elastic-plastic displacement. As the LGT deformation becomes larger, the drag force during insertion of the RCCA increases. To establish the limit cross-flow load that allows the RCCA insertion, a mockup mechanical test was carried out.

1.3 Guide Tube Design Arrangement

Figure 1.3-1 shows the GT configuration. The GT has two main assemblies; an UGT and a LGT. The GT flanges are fastened together by bolts threaded to the top of the upper core support plate. The LGT is inserted through the holes in the upper core support plate and restrained in the horizontal direction by a small clearance between the LGT flange and upper core support plate hole. The bottom of the LGT is fastened by two large support pins with flexible leaves that can slide vertically with a small amount of friction force, but are horizontally preloaded against the upper core plate holes to prevent excessive vibration and wear. The UGT and LGT have the guide plates that lead the control rod spider during insertion and retraction of the RCCA. The LGT has a continuous section of C-tubes and sheaths just above the upper core plate hole that prevents excessive vibration of the RCCA from fuel assembly reactor coolant flow. The LGT also has “windows” to allow the flow to egress to the plenum between the upper core support and upper core plate. As shown in Figure1.3-1, the LGT is subjected to the primary coolant flow towards the outlet nozzles. At the LOCA event, as a hot leg pipe is broken, the flow rate at the outlet increases rapidly. This causes abnormally high cross-flow loading on the LGT located near the outlet nozzle. There is a possibility that the LGT deforms plastically depending on rupture pipe size. This means that the LGT may have a permanent displacement after the postulated LOCA event. As a result, the drag force could increase as the RCCA passes through the LGT and impede the RCCA into the core.

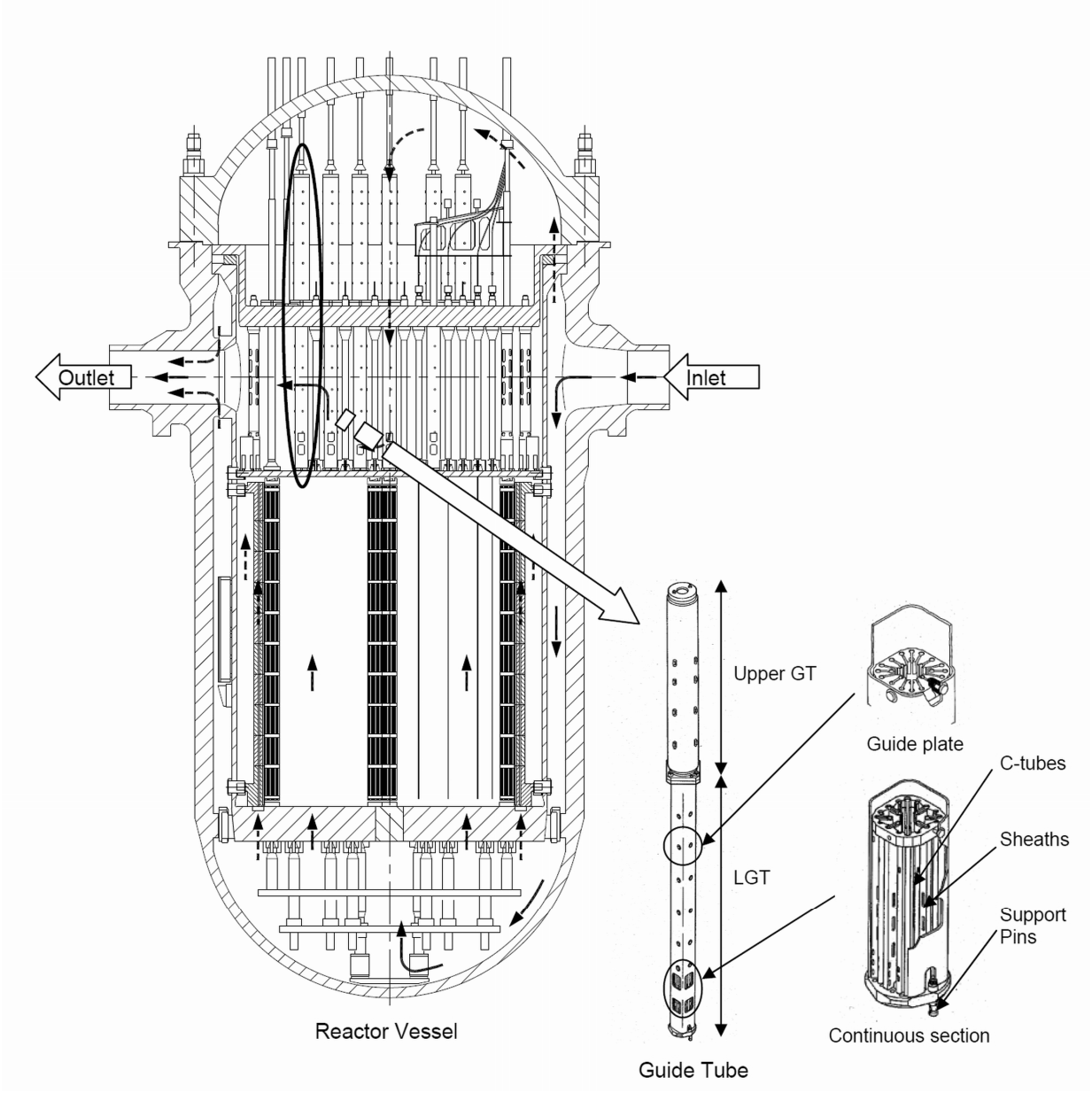

Figure 1.3-1 Guide Tube (GT) Configuration and Reactor Coolant Flow Path under Operation

1.4 Process of Determining RCCA Insertion Limit Load

In the RCCA insertion test, multiple concentrated loads equivalent to the cross-flow load distribution in the actual plant were applied on the mockup of LGT. The purpose of the test was to obtain the correlation between the elastic-plastic deflection of the LGT and the quasi-static RCCA insertion drag force profile at RT. Using this test result, the computational simulation of the RCCA insertion was conducted to determine the limiting displacement or permanent set after the LOCA event that allows the RCCA to be dynamically inserted. In this analysis, the insertion drag force was input by multiplying the measured drag force by the ratio of the Young's modulus for the RCCA material at the operating temperature to that at the RT. By using the elastic-plastic FEA results, the load that produces the limiting displacement of the LGT was determined as the RCCA insertion limit load at the operating temperature. Figure 1.4-1 shows the evaluation flow of the RCCA insertion limit load.

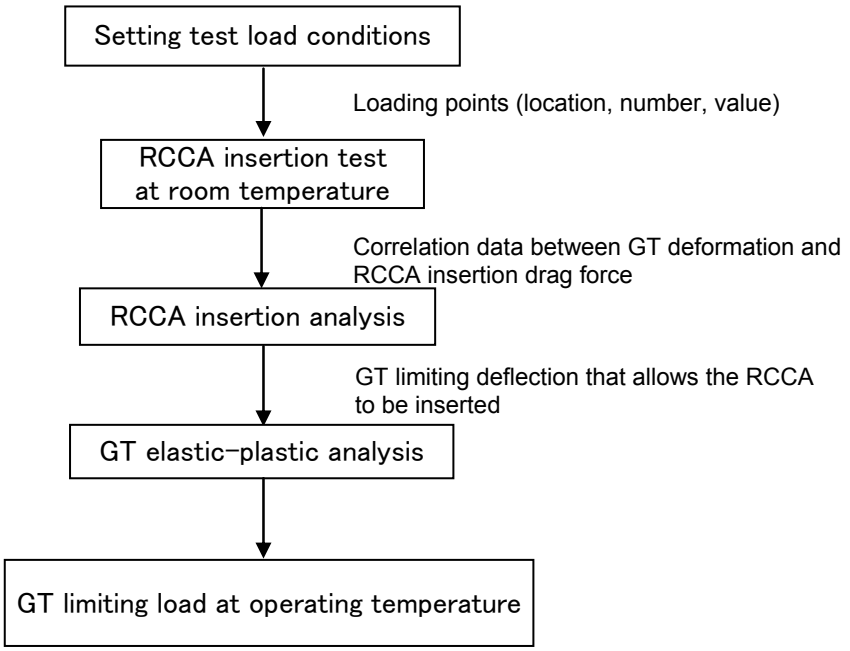

Figure 1.4-1 Process of Determining RCCA Insertion Limit Load

2. Determination of Test Load Conditions

2.1 Setting Process

The actual cross-flow load on the LGT during the plant operation is distributed non-uniformly in a longitudinal direction. However, it is complicated to simulate the actual distributed load in the mockup test; therefore, an equivalent concentrated loading with multiple loading points can be generated. Because the RCCA insertion drag force is directly affected by the LGT deformation, it is very significant to set the loading conditions including loading the point locations, the number of loading points, and multiple concentrated load amounts such that the horizontal LGT displacement simulates that of the actual distributed loads. In addition, aiming at the load control during the test, it is preferred that the number of loading points is minimized. To determine the appropriate test conditions, the static FEA with a general purpose finite element code of “ABAQUS” was conducted for both the distributed and the concentrated loads. Comparing those analysis results, the equivalent concentrated load conditions including the loading point locations, the number of loading points, and the load distribution ratio were determined. Next, to determine the displacement of each loading point, with keeping the load distribution ratio, the load amount at each loading point was increased step by step. By this elastic-plastic FEA, the displacement of LGT at each loading point was obtained. The process summary of deciding the test conditions is shown in Figure 2.1-1.

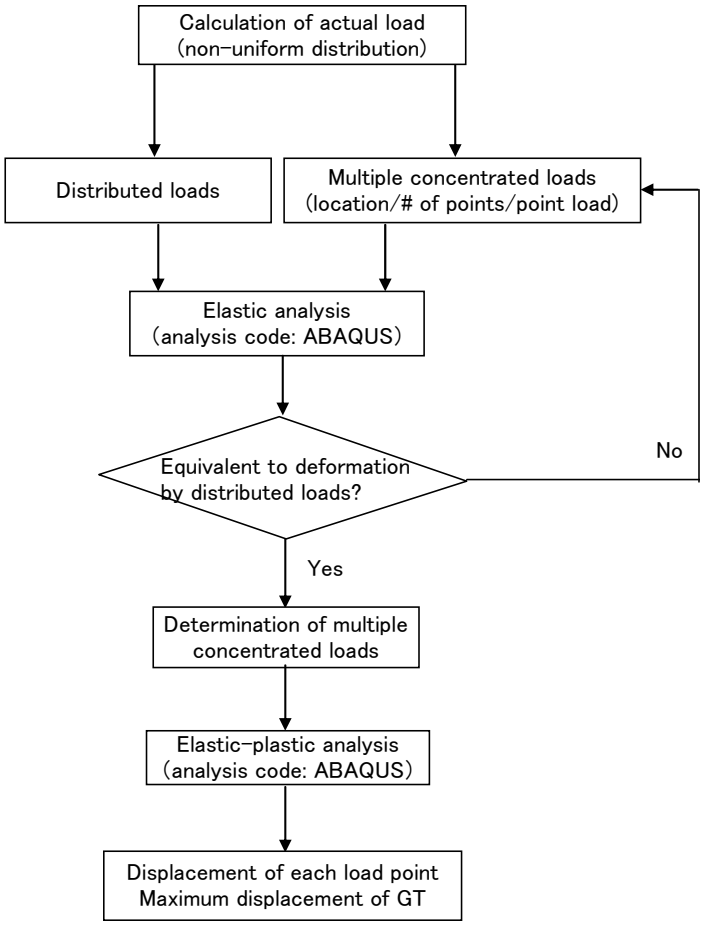

Figure 2.1-1 Process for Determining the Test Load Conditions

2.2 Test Load Conditions

2.2.1 Methodology of Cross-flow Load Calculation

The cross-flow towards the outlet nozzle applies the highest loading on the LGT. The load distribution was obtained by calculating the flow in the upper plenum based on the potential flow theory. In the calculation, it was considered that the inlet flow comes from the reactor core and the outlet flow egresses towards the outlet nozzle. The flow velocity distribution was determined by numerically solving the theoretical simultaneous equations for incompressible flow. The fundamental equations are as follows. (Ref. (1))

Using the velocity potential Φ, the continuity equation for the incompressible fluid is expressed in cylindrical coordinates as

$$\frac{1}{r}\cdot\frac{\partial}{\partial r}\left(r\cdot\frac{\partial\Phi}{\partial r}\right)+\frac{\partial^2\Phi}{\partial z^2}+\frac{1}{r^2}\cdot\frac{\partial^2\Phi}{\partial\theta^2}=0$$

The velocity is expressed as

$$\vec{V}=-\nabla\Phi \qquad \left(ie.\ V_r=\frac{\partial\Phi}{\partial r},\ V_\theta=\frac{\partial\Phi}{r\cdot\partial\theta},\ V_z=\frac{\partial\Phi}{\partial z}\right)$$

The boundary conditions of the upper plenum are descried below.

Where,

Φ : The velocity potential
V : The flow velocity
V_{ei} : The flow velocity at the outlet nozzle
r_1 : The radius of the upper plenum
L : The height of the upper plenum

The load is calculated by converting the flow velocity into the load. The cross-flow load applied to the LGT ($F(z)$) is defined as the normalized load. The cros-flow load in the horizontal direction per unit length is expressed as the ratio between the squared flow velocity and the squared maximum velocity because the load is proportional to the square of the velocity. The entire load distribution of the LGT was determined by accumulating the load per unit length.

$$F(z) = \frac{V^2(z)}{V_{\max}{}^2}$$

Where,

$F(z)$: The normalized load per unit length
$V(z)$: The flow velocity $\sqrt{V_r{}^2 + V_\theta{}^2}$
V_r : The velocity in the radial direction
V_θ : The velocity in the circumferential direction

2.2.2 Applied Load to LGT

Figure 2.2-1 shows the actual non-uniform load distribution that is expected to apply to the LGT. The maximum value of it is normalized as “1”. The target LGT is the one located the nearest the outlet nozzle (cf. Figure 2.2-2). The vertical axis is the distance from the top surface of the upper core plate. The equivalent [ ] concentrated loads are expressed as the ratio to the maximum value in Figure 2.2-1.

The comparison result of the LGT displacement between the distributed load and [ ] concentrated loads is plotted in Figure 2.2-3. This figure shows the relationship between the horizontal displacement of LGT (horizontal axis) and the distance from the bottom of the LGT (vertical axis). Furthermore, the [ ] concentrated loads were applied at the level of the stiff guide plates to prevent the LGT enclosure shell from locally deforming. As shown in Figure 2.2-3, it is confirmed that the cross-flow distribution loading can be simulated suitably by the [ ] concentrated loads. That is, the LGT deformation with the [ ] concentrated loads is equivalent to that with the cross-flow distribution load. Next, using the elastic-plastic FEA, the displacement of LGT at each loading point was determined for each maximum displacement in the range of [ ] in. to [ ] in. with the increment of [ ] in. keeping the distribution ratio of the [ ] concentrated loads. The sample of the LGT deformation is shown in Figure 2.2-4, and the displacement of the load point for each step is listed in Table 2.2-1. These values are used as the test load conditions for the RCCA insertion test.

Figure 2.2-1 Comparison of Actual Distributed Load and Equivalent Concentrated Load

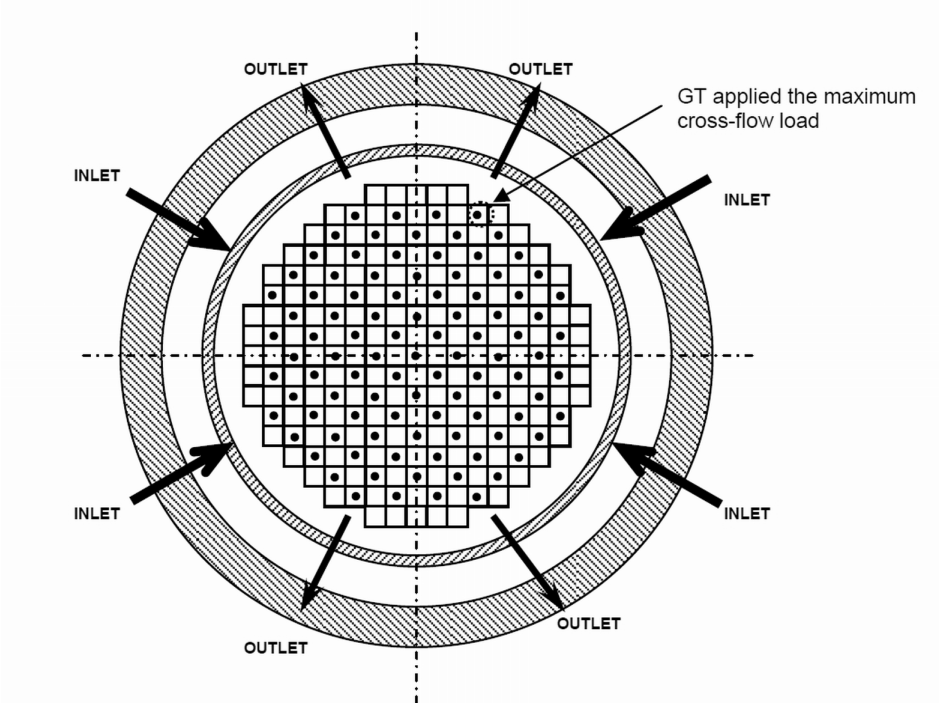

Figure 2.2-2 Location of the LGT Applied the Maximum Cross-flow Load

Figure 2.2-3 LGT Deformation Comparison between Actual Distributed Load and [ ] Concentrated Loads

Figure 2.2-4 Sample LGT Deformation due to Various Cross-flow Loads

Table 2.2-1 Applied Displacements at Loading Points for Each Maximum Displacement of LGT

Maximum displacement of LGT [in.]	Applied displacement at loading point [in.]

3. TEST METHODOLOGY

To obtain the correlating data of the load, the LGT deformation, and the RCCA insertion drag force, the mechanical test was performed using the mockup that simulates the whole of the actual RCCA drive-line. As described in the previous section, the actual cross-flow load on the LGT is replaced by [ ] equivalent concentrated loads. The RCCA was inserted from the upper side of the LGT to measure its insertion drag force deforming the LGT step by step. Until the material characteristic of the LGT is reached its plastic region, the loading-unloading-loading process was repeatedly performed.

3.1 Test Apparatus

The outline of the test apparatus is shown in Figure 3.1-1.

3.1.1 Driveline

To obtain the RCCA insertion drag force, it is necessary that the configuration, rigidity, and friction of the entire mockup simulate those of actual driveline adequately. The LGT, FA skelton, RCCA, and drive rod assembly that comprise the RCCA driveline were provided to be the same as the actual one. The CRDM was simplified by use of a plain pipe whose cross sectional shape is the same as the actual one because there is a possibility that the drive rod assembly could contact the inner surface of the CRDM due to large deformation of the LGT. This change has no effect on the LGT deformation results in the test.

3.1.2 Others

The other structural components supporting the driveline in this test are the upper core support plate, upper core plate, and lower core support plate. The thickness of these mockups was made to be the same as the actual components to fully reproduce the supporting structure and strength. The trestles around the driveline mockup were designed to be rigid enough to withstand the excessive load that may apply to it during the test.

3.1.3 Loading Mechanism and Conditions

The concentrated loads were applied to the external surface of the enclosure at [ ] levels that the intermediate guide plates are positioned. The loading device was controlled to match the measured displacement at the loading points with the targeted displacement listed in Table 2.2-1. To obtain the relationship between the insertion distance and the RCCA insertion drag force, the RCCA mockup was moved downward in the quasi-static manner. To evaluate the test on the safety side, the loading was applied in the direction of 45 degrees as shown in Figure 3.1-2 because the LGT most likely yields in this direction due to its lower modulus of section. The loading jig was designed to be L-shaped to minimize any local deformation of the LGT enclosure. The LGT was displaced in [ ] in. increments until the RCCA insertion drag force becomes larger than the insertion force. For each loading condition, the RCCA insertion drag force was measured. The RCCA insertion speed was well-controlled so that the insertion speed does not affect the inertial force at the time of ‘insertion stick’.

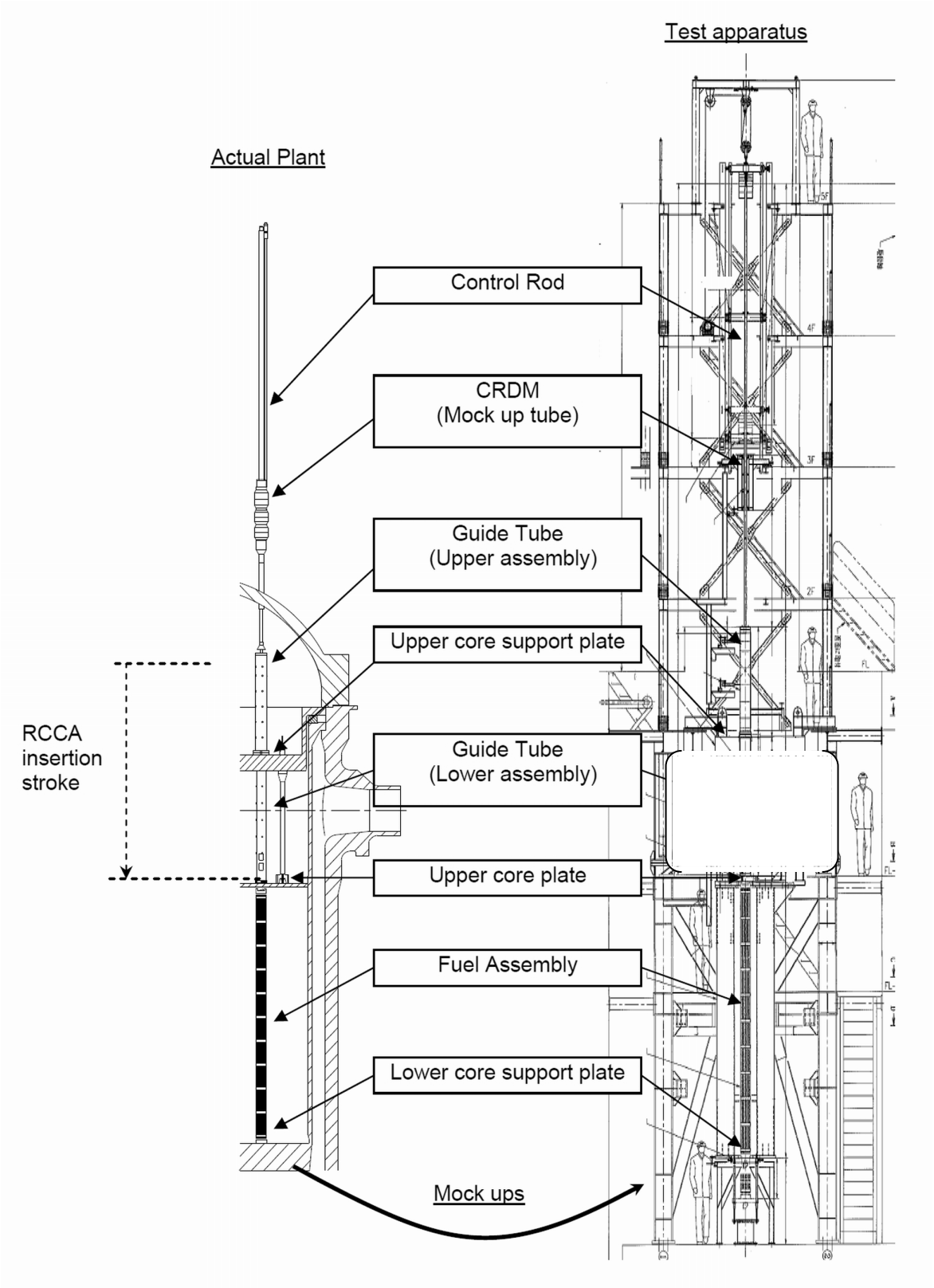

Figure 3.1-1 Test Apparatus

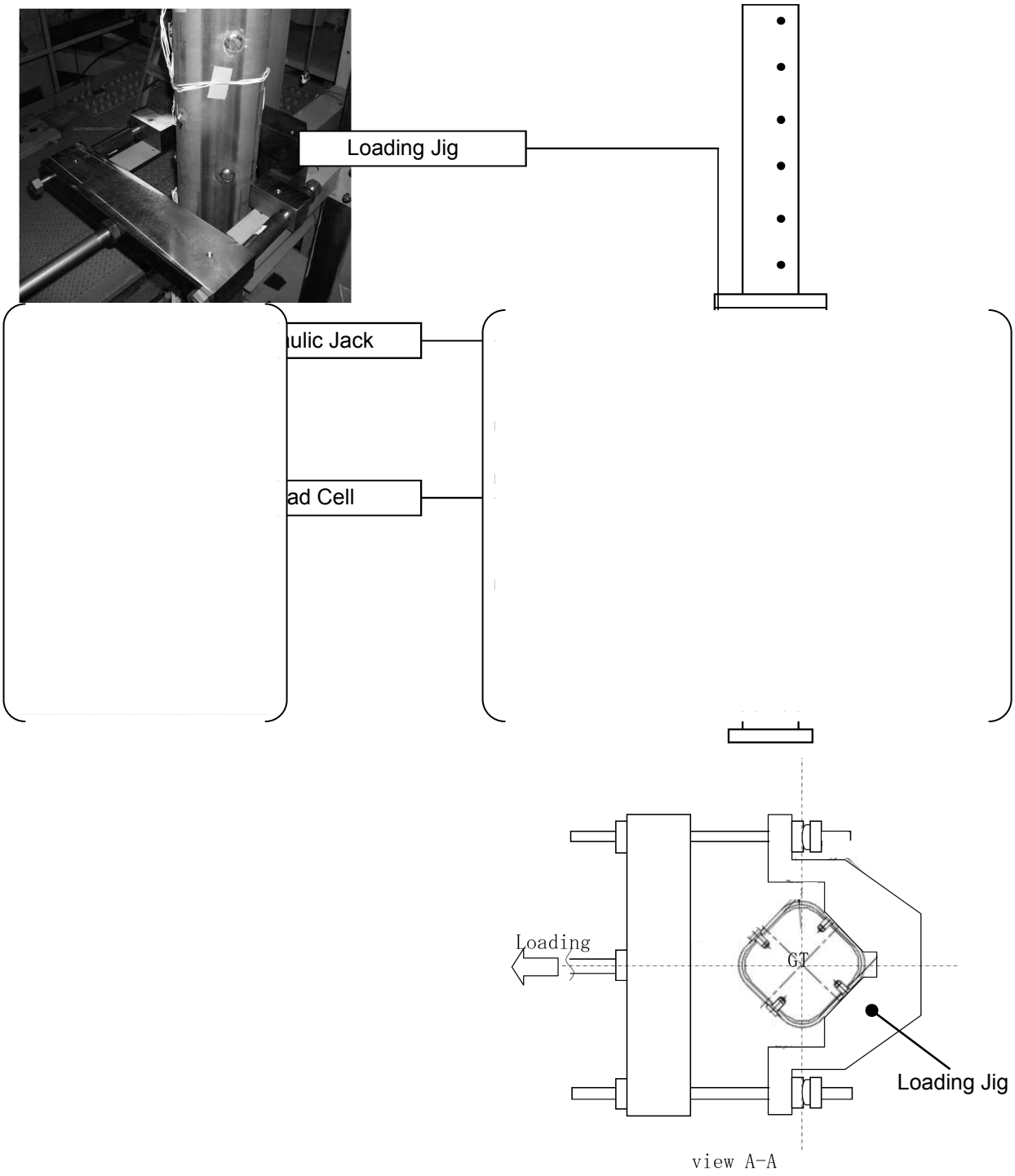

Figure 3.1-2 Loading Mechanism

3.2 Measurements

3.2.1 Measuring Items

The items listed in Table 3.2-1 were mainly measured. The block diagram of the measurement system is shown in Figure 3.2-1, and the measuring points are shown in Figure 3.2-2. The reaction force in the vertical direction was measured as the RCCA was quasi-statically inserted. The measured reaction force is defined as the RCCA insertion drag force. Based on the measured LGT displacements and RCCA insertion drag force, the insertion drag force profile was plotted for the entire insertion range. To visualize the test results, the correlation of the LGT's loading and the displacement was also graphically illustrated.

Table 3.2-1 Measuring Items

Measuring item	Measuring device	Direction	Measuring point(*)	Quantity
Loading applied to GT	load cell	horizontal	○	
GT displacement	displacement gauge	horizontal	△	
RCCA insertion distance	displacement gauge	vertical	●	
RCCA incertion drag force	load cell	vertical	▲	
GT strain	strain gauge	vertical	■	

(*) Refer the marks to Figure 3.2-2

Figure 3.2-1 Block Diagram for Measurement System

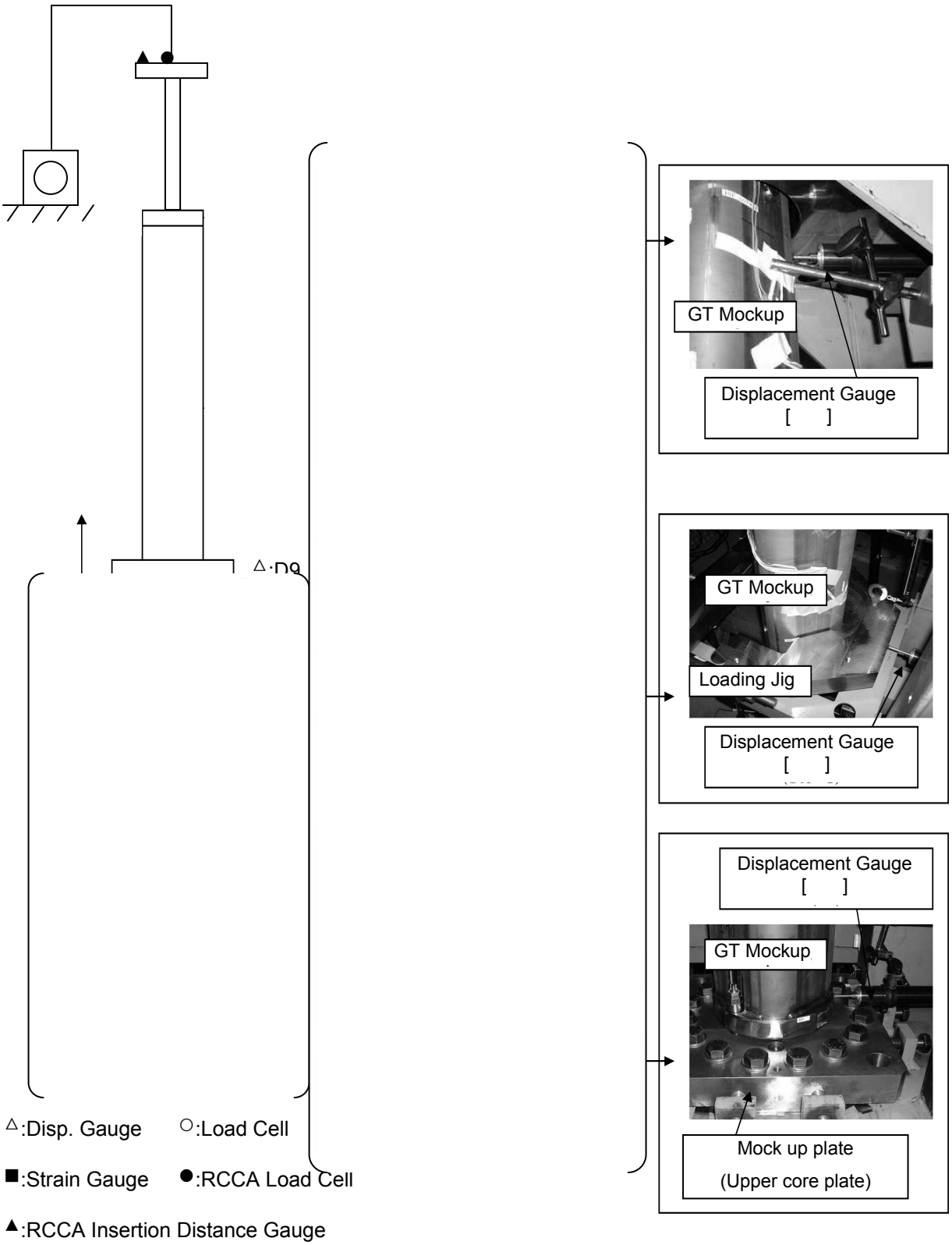

Figure 3.2-2 Measuring Points

3.3 Test Procedure

The test procedure is shown in Figure 3.3-1. During the phase1, the RCCA was quasi-statically moved downward, and its insertion drag force was measured. The loaded LGT restores to original state with a spring-back effect after unloading as far as the load is applied to the LGT in the elastic region. It should be noted that the safety requirement is to ensure that the RCCA can be inserted after the LOCA event, since RCCA insertion may fail during the maximum LOCA loading. When the RCCA was not able to be inserted after loading, the RCCA was inserted after unloading only to acquire data of the drag force per insertion distance. (phase2)

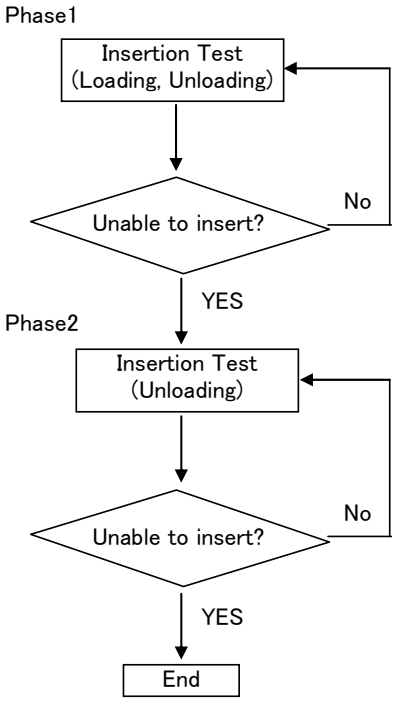

Figure 3.3-1 Test Procedure

4. TEST RESULTS AND EVALUATION

4.1 LGT Load Displacement Curve

Figure 4.1-1 illustrates the load displacement curve. The horizontal axis is the maximum displacement of the LGT; whereas, the vertical axis is the total load that is the sum of [ ] concentrated loads. After loading at the points with the circles shown in Figure 4.1-1, the RCCA insertion drag force was measured. And then, after the applied loads on LGT were released, the RCCA insertion drag force was measured again without the loads at the points with the triangles. This loading and unloading test scheme was used in the analysis of each test case.

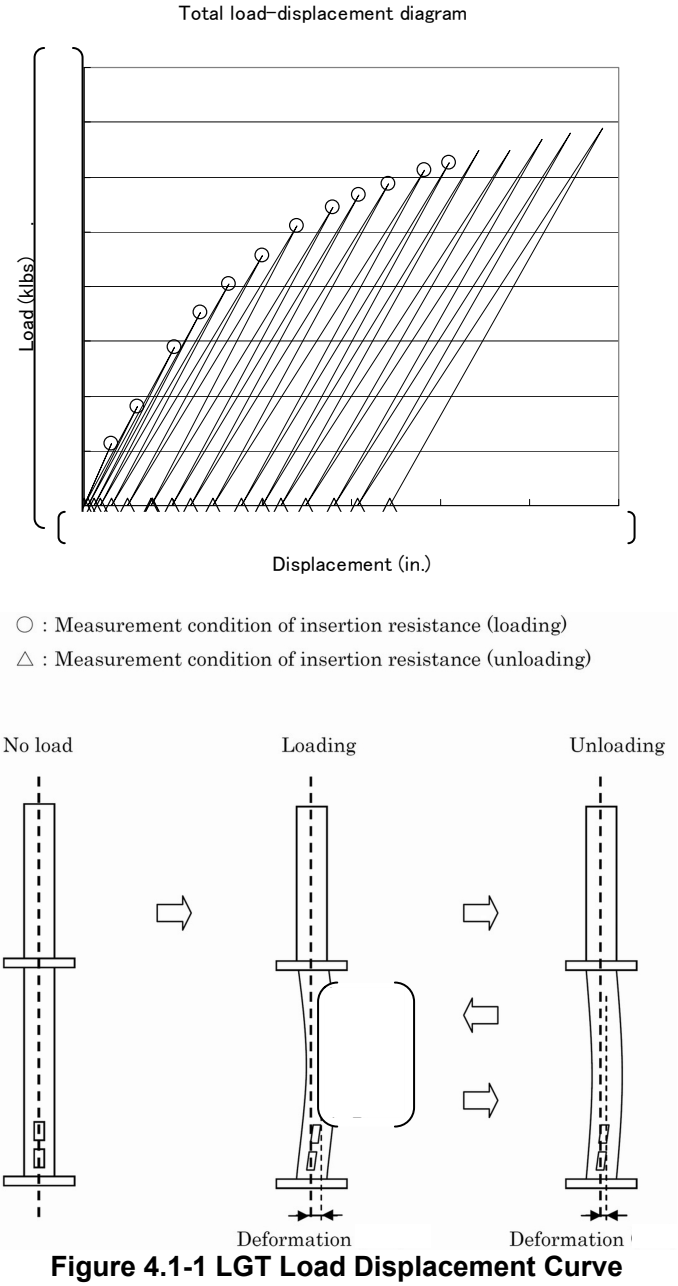

Figure 4.1-1 LGT Load Displacement Curve

4.2 LGT Displacement

Figure 4.2-1 is the test result of LGT deformation for the case No.22 where the maximum displacement was [ ] in. after loading. The measured LGT displacement result shows that the LGT is locally deformed at the loading points; however, the measured strain result of the LGT surface shows the smooth distribution. The reason for this is that the LGT is locally deformed at the jig's contacting surface with the load, and the local deformation is measured as the displacement of the LGT. The distribution of the LGT displacement was estimated based on the measured strain in absence of the jig's effect. This distribution curve was well-fitted to the actual LGT displacement except the loaded points, and the large displacements were measured at D4 and D6. Hence, the measuring point D5 which is located in between these points is defined as the maximum displacement point. Based on the measured data of the point D5, the maximum LGT displacements for each test case were summarized in Table 4.2-1.The test case 1 through 3 is the test results of the LGT displacements under the unloading condition which were conducted to confirm the repeatability of the test apparatus. The test case 4 through 30 is the test results of the LGT displacements under the loading-unloading condition. In the test case 30 under the loading condition, the RCCA was not inserted with the specified maximum load for this test which was applied to the top of the RCCA; therefore, the measurement of the RCCA drag force under the loading condition was terminated. The test case 31 and the later are the test results under the unloading condition.

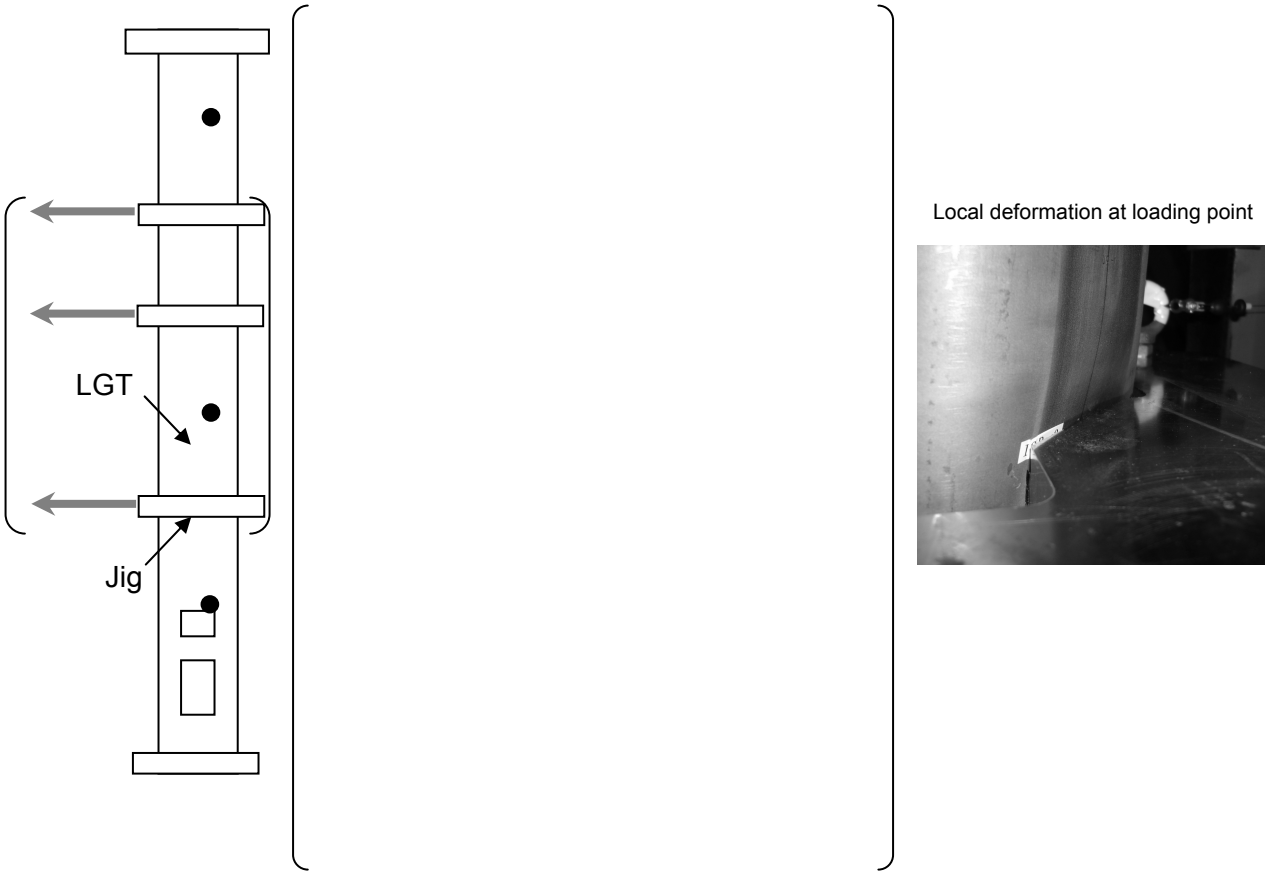

Figure 4.2-1 Measured LGT Displacements and Strains

Table 4.2-1 Maximum Displacements of LGT (at the measuring point D5)

Test case	Maximum displacement amount (in.)	Test case	Maximum displacement amount (in.)
1		22	
2		23	
3		24	
4		25	
5		26	
6		27	
7		28	
8		29	
9		30	
10		31	
11		32	
12		33	
13		34	
14		35	
15		36	
16			
17			
18			
19			
20			
21			

4.3 RCCA Insertion Drag Force

Figure 4.3-1 and Figure 4.3-2 show the relationship between the LGT displacement and the RCCA insertion drag force. The comparison of case22 and case28 implies that the increment of the LGT displacement increases the RCCA insertion drag force. Especially, the RCCA insertion drag force becomes larger around the continuous section of LGT which creates larger friction between the RCCA and the LGT. This arises from the structural property of the continuous that is designed to be an un-separated straight guide with high rigidity.

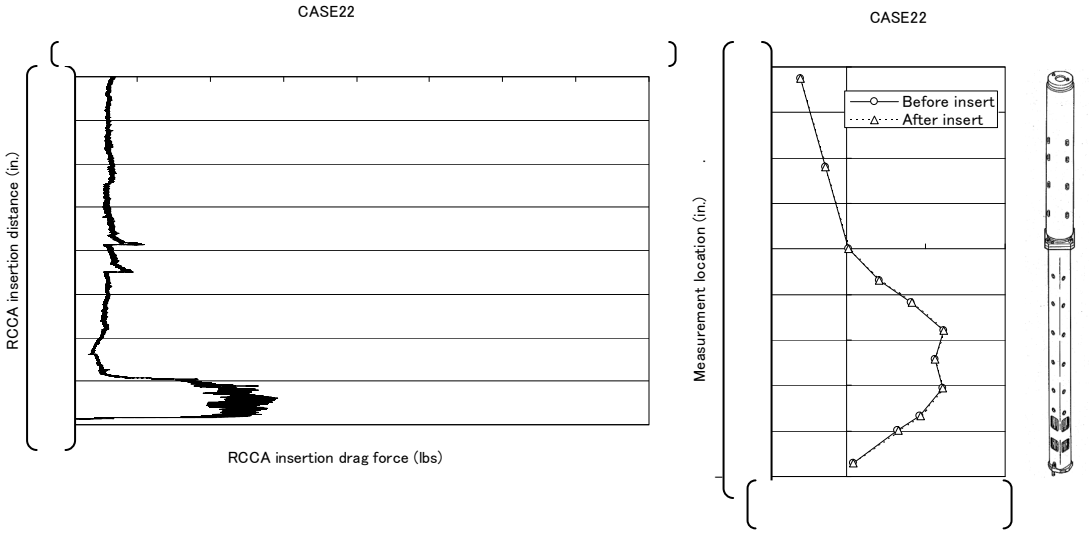

Figure 4.3-1 LGT Displacement and RCCA Insertion Drag Force (case22)

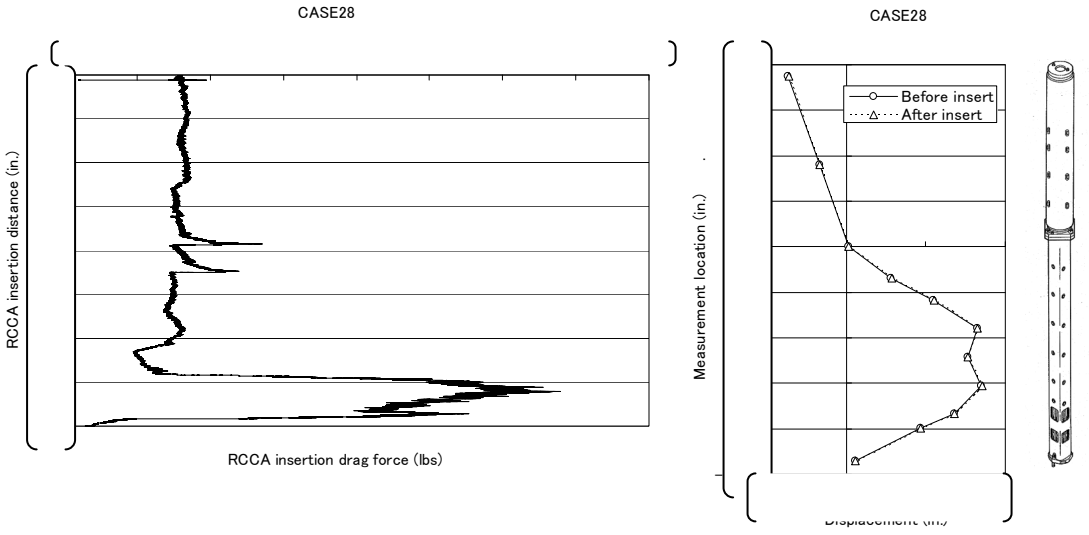

Figure 4.3-2 LGT Displacement and RCCA Insertion Drag Force (case28)

4.4 LGT Displacement Limit for RCCA Insertion

As the consequence of the RCCA insertion drag force increase, the RCCA insertion speed is lowered. The free fall motion of the actual RCCA under the operational conditions can be expressed equation (1) below. The RCCA insertion drag force is included in the mechanical drag force (F_m) on the right hand side of the equation. Using the insertion drag force profile measured in the test, as shown in Figure 4.3-1 and Figure 4.3-2, the maximum LGT displacement that allows the RCCA to be inserted (=RCCA insertion limit) was specified. Based on the fact that the flexible RCCA deforms elastically in this test range, the RCCA insertion drag force was compensated by multiplying the ratio of the 'Young's modulus' at operating temperature and RT. Figure 4.4-1 shows the time needed to fully insert the RCCA associated with the LGT deformation. In this figure, the RCCA insertion time at the initial condition is set as '1', and the other insertion times are normalized with respect to the initial insertion time. The RCCA insertion analysis result is summarized in Table 4.4-1. Thus, the LGT displacement limit for the RCCA insertion under the unloading condition was determined as [ ] in. at the operating temperature of 617°F.

$$M \cdot \frac{d^2x}{dt^2} = M \cdot g - (F_f + F_m + F_u) \qquad \ldots(1)$$

Where,

$M \cdot g$: Internal force due to the acceleration of gravity of RCCA + drive rod assembly

F_f : Hydraulic drag force

F_m : Mechanical drag force

F_u : Buoyancy force

x : RCC Insertion distance

t : Insertion time

Table 4.4-1 RCCA Insertion Analysis Results

Test condition	LGT Maximum displacement (in.)	RCCA insertion
unloading	[ ]	YES
unloading	[ ]	NO

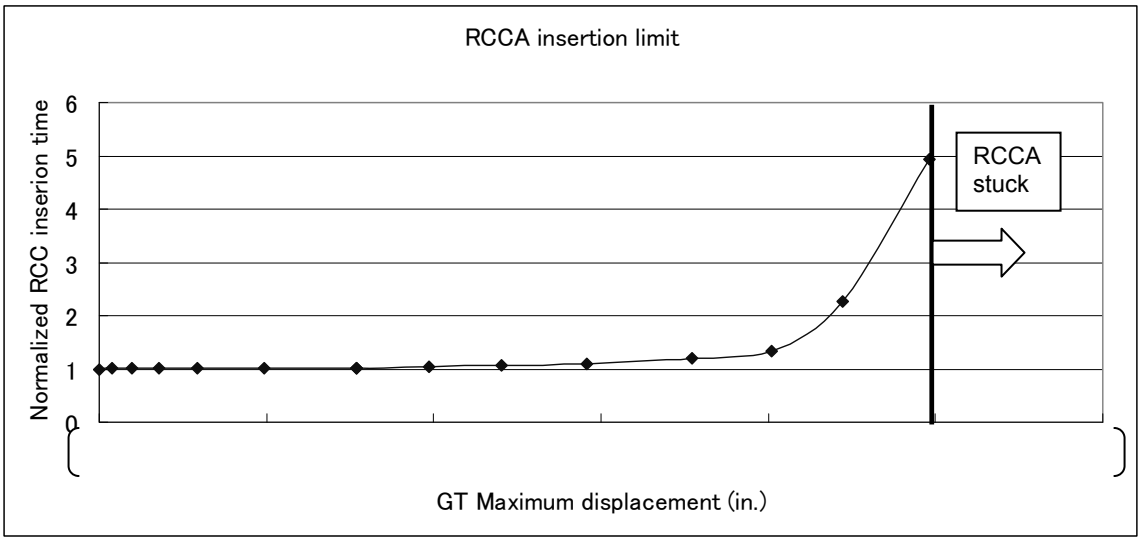

Figure 4.4-1 Maximum Displacement of LGT and RCCA Insertion Limit under Unloading Condition

5. RCCA INSERTION LIMIT LOAD

5.1 Procedure

The RCCA insertion limit load on the LGT is estimated to be [ ] lbs at the limiting displacement [ ] in. from the load displacement curve shown in Figure 4.4-1. However, the load displacement curve was obtained from the test at RT. The limit load at the operational temperature decreases because the mechanical material properties differ from those at RT. The elastic-plastic FEA was conducted to determine the RCCA insertion limit load at the operating temperature. First, the FE model of the LGT mockup was created with a solid element. A non-linear stress-strain curve at RT obtained from tensile test specimens which were extracted from the LGT mockup was used as the material property in the FEA. To validate the analysis method, a benchmark analysis was run under the same conditions as the mockup test, and the analysis results were compared with the test measurements. Next, the load on the LGT that allows the RCCA to be inserted at the operating temperature was determined using the stress-strain curve that was similarly obtained from the tensile test specimens at high temperature. That is, the load that deforms the LGT [ ] in., which is the RCCA insertion limit, under the unloading condition was determined at the operating temperature. The determination process of the RCCA insertion limit load at the operating temperature is shown in Figure 5.1-1.

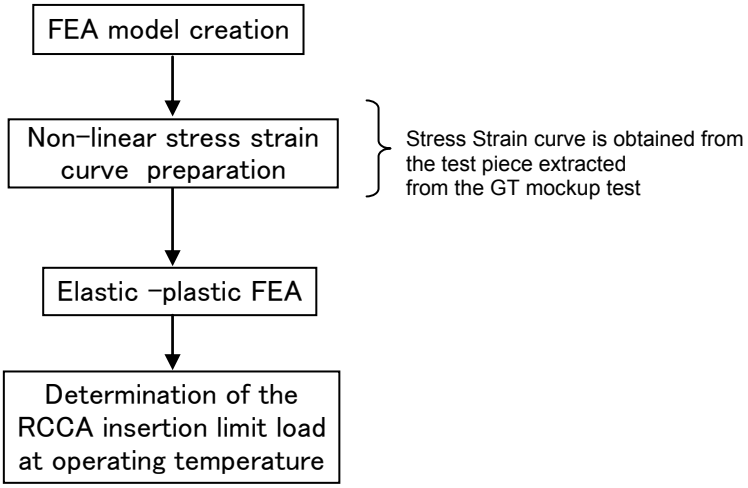

Figure 5.1-1 RCCA Insertion Limit Load Determination Process

5.2 Elastic-plastic Analysis

5.2.1 LGT Analysis Model

The FE model was precisely created from the middle flange to the bottom flange of the LGT as shown in Figure 5.2-1. The element type was hexahedral (ABAQUS element: [ ]) with the meshed [ ] elements and [ ] nodes. [

]

5.2.2 Stress-Strain Curve

Figure 5.2-2 and Figure 5.2-3 are the measured Type 304 stainless steel stress-strain curves at RT of 70^{o}F and hot temperature of 617^{o}F, respectively. Four tensile test specimens for the RT and hot temperature conditions were taken from the actual LGT enclosure material used in the test mockup.

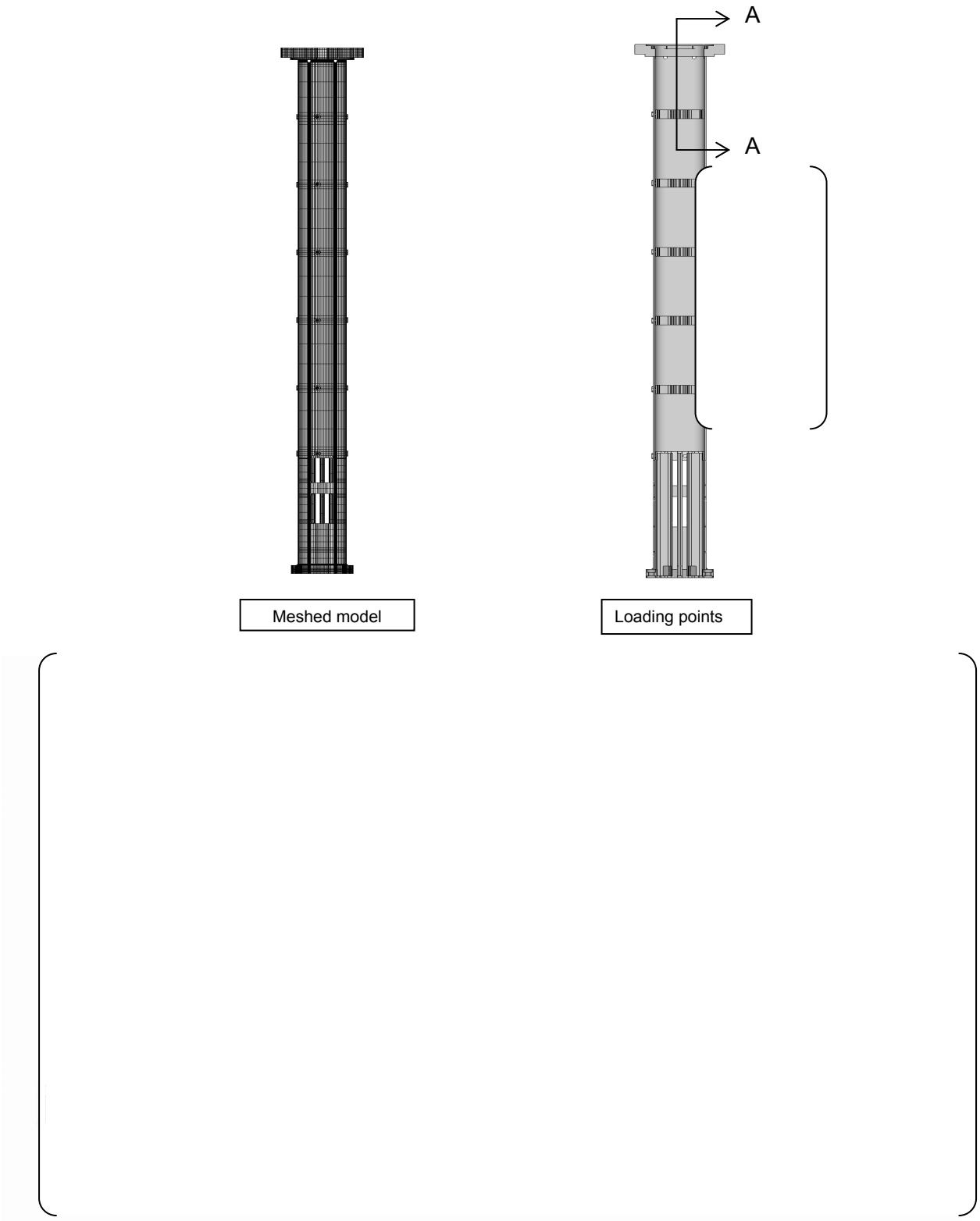

Figure 5.2-1 FE Model

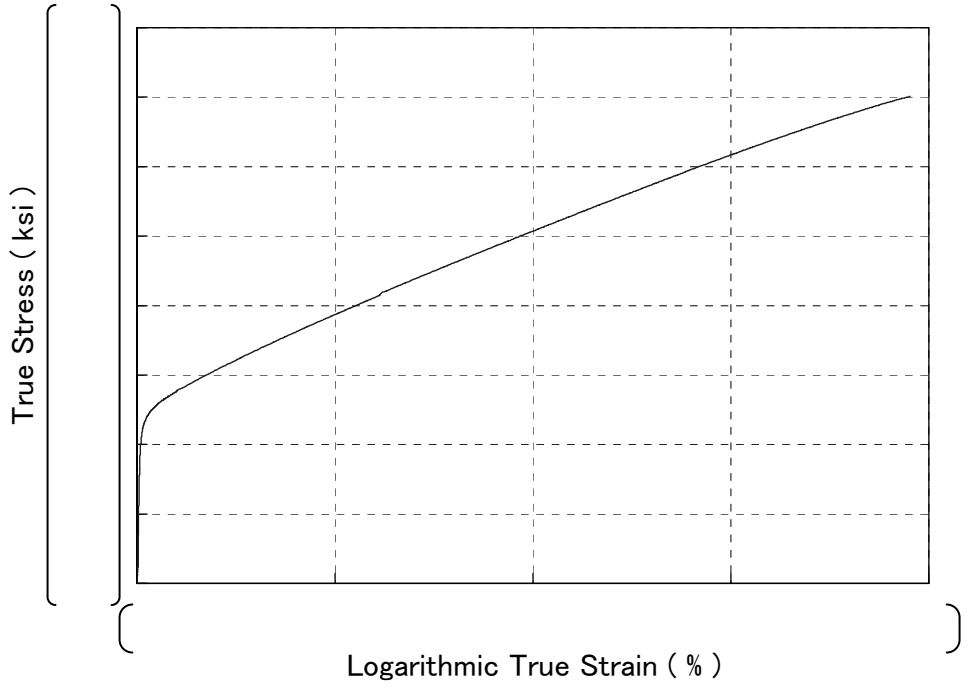

Figure 5.2-2 Stress-strain Curve at RT 70°F for Type 304 Stainless Steel

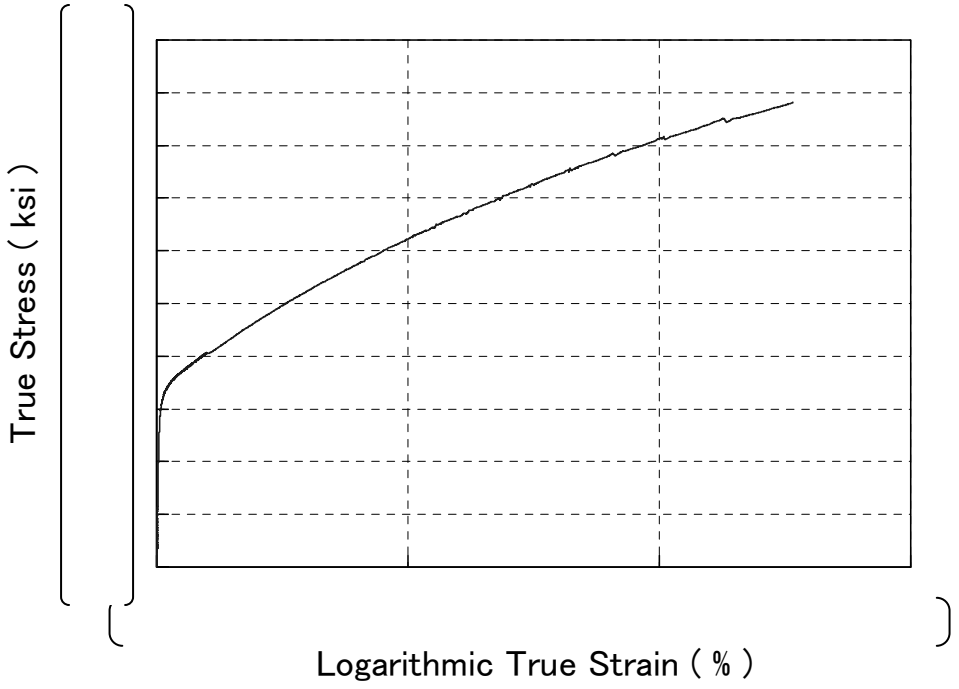

Figure 5.2-3 Stress-strain Curve at 617°F Operating Temperature for Type 304 Stainless Steel

5.2.3 Validation of FE Method

(1) Comparison of Load Displacement Curves

Using the FE model (Figure 5.2-1) and the stress-strain curve (Figure 5.2-2), the FEA was conducted to simulate the LGT deformation at RT. Figure 5.2-4 shows the FEA result of the LGT compared with the test result. The load is the sum of the [ ] concentrated loads, and the maximum displacement is measured at the measuring point D5. As a result, it was confirmed that the FEA result successfully matched with the test result.

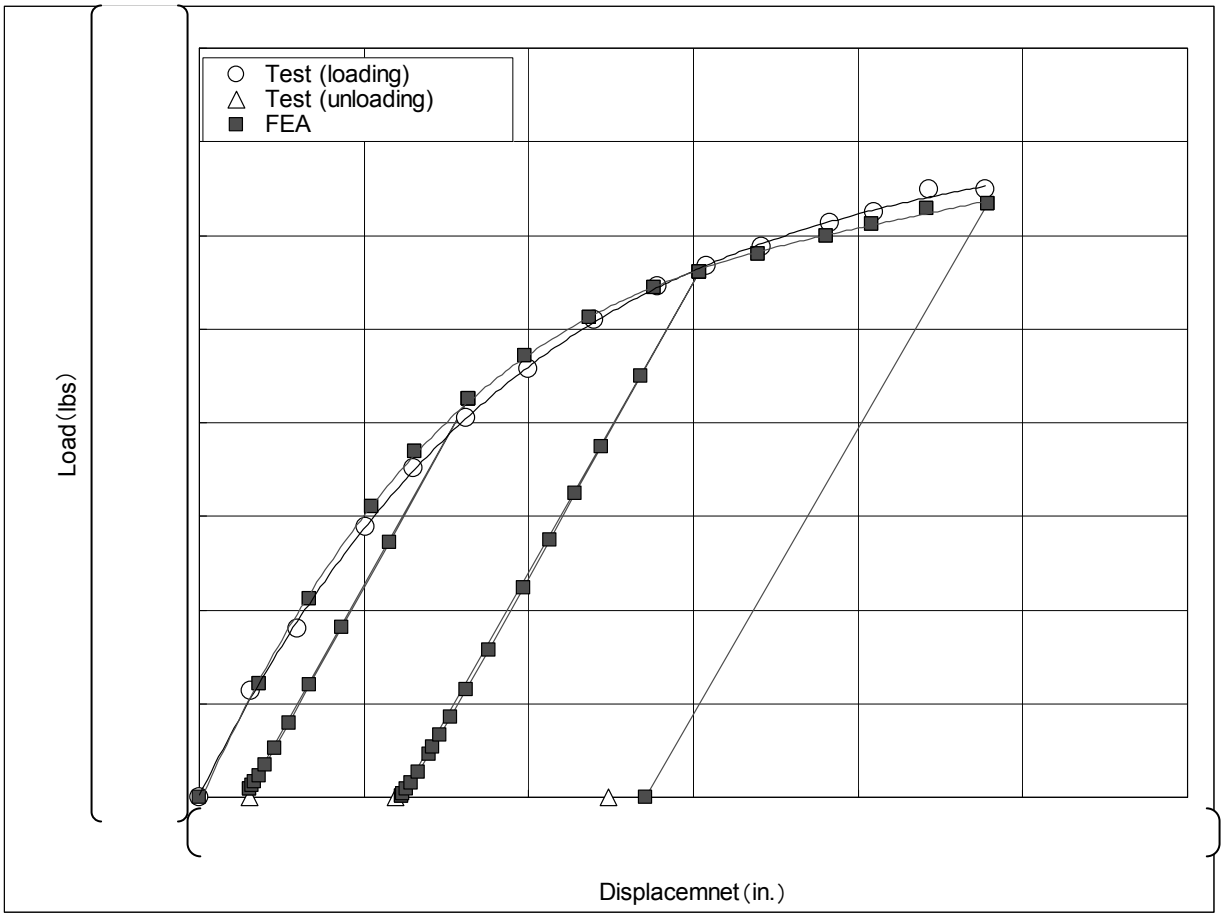

Figure 5.2-4 Analysis Model Benchmarking Result at 70°F

(2) Comparison of LGT Displacements

For test cases 22 and 28, the FEA results of the LGT displacements are compared with the test results shown in Figure 5.2-5. For the displacements, it was confirmed that the FEA results successfully matched the test results. Thus, the FEA precisely simulates the elastic-plastic characteristic of the LGT under the loading and unloading test conditions.

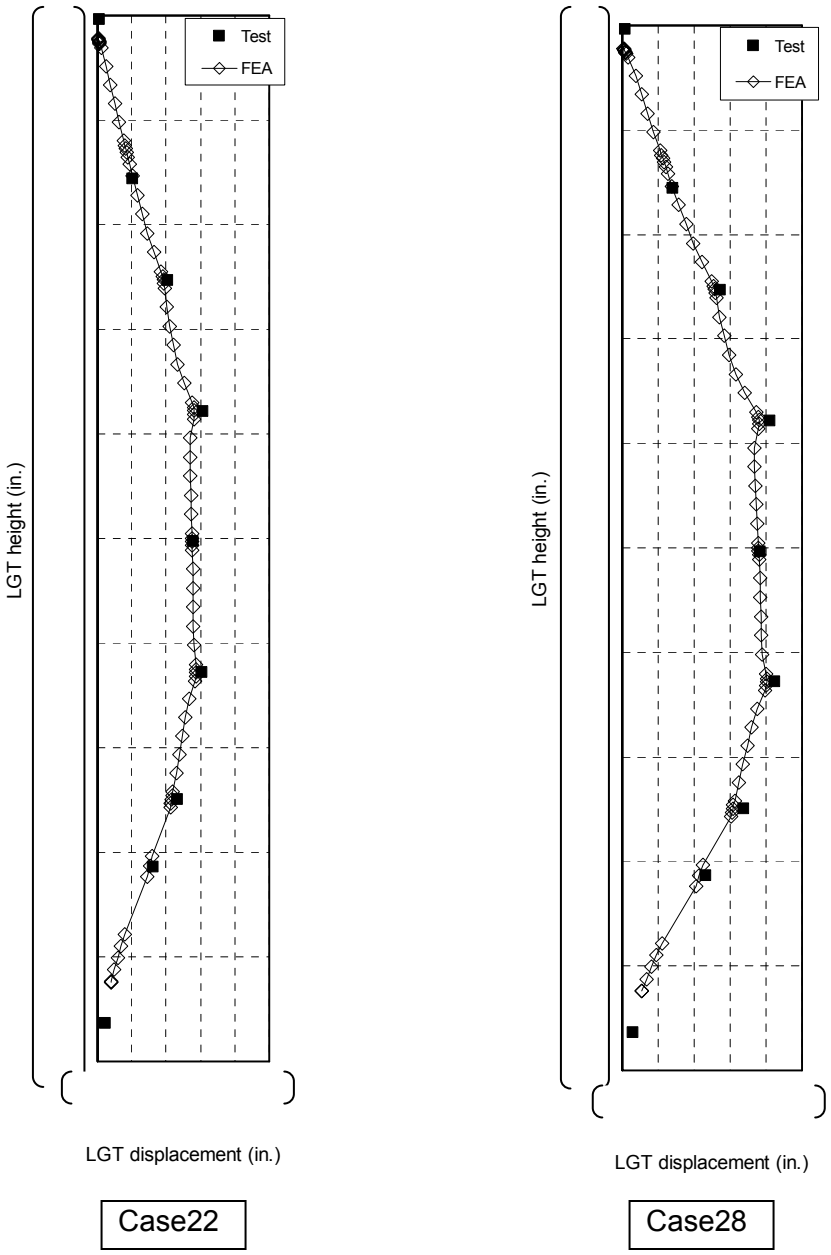

Figure 5.2-5 LGT Horizontal Displacements at RT for Case 22 and Case 28

5.2.4 Determination of LGT Insertion Limit Load at Operating Temperature

Using the stress-strain curve shown in Figure 5.2-3, the FEA was conducted to simulate the LGT deformation at the operating temperature of 617°F. Figure 5.2-6 shows the FEA result of the load-displacement curve. By using the slope of the elastic line plotted under the unloading process, the limiting load that allows the RCCA to be inserted was graphically determined. This load of [ ] lbs. is the RCCA insertion limit load at the operating temperature. As compared to RT described in the previous section 5.1, the RCCA insertion limit load is reduced by approximately [ ] % at the operating temperature.

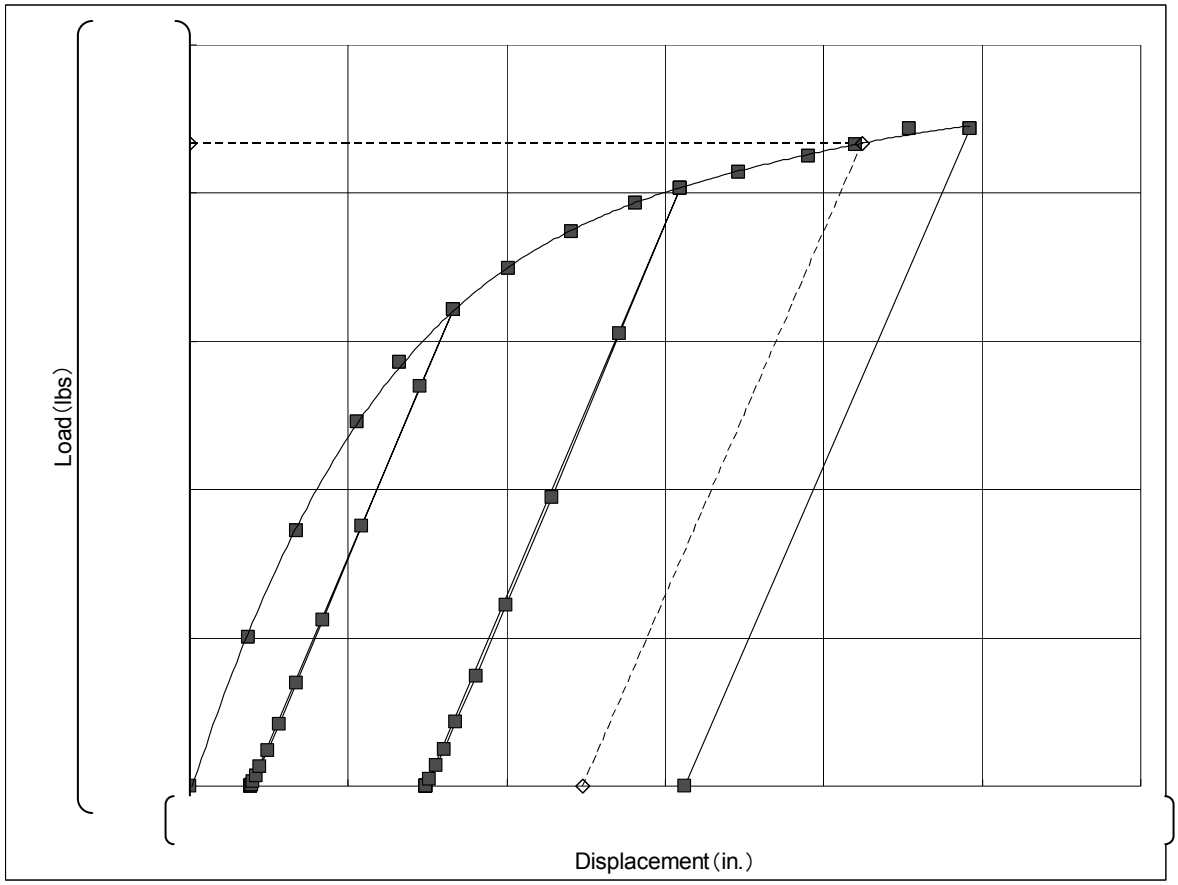

Figure 5.2-6 Determination of the LGT RCCA Insertion Limit Load at 617°F

6. CONCLUSIONS

From the results of the RCCA insertion limit load test for US-APWR, the following conclusions are drawn:

(1) The RCCA insertion limit load at the operating temperature is [ ] lbs.

(2) It can therefore be concluded that when the maximum LOCA loading is less than the RCCA insertion limit load of [ ] lbs, the RCCA can be inserted without impediment through the LGT after the postulated LOCA event.

7. REFERENCES

(1) Ronald L. Panton (1995). Incompressible flow (2nd edition). Austin, Texas: John Wiley & Sons Canada, Ltd.